

Diffusion-weighted endorectal MR imaging at 3T for prostate cancer: correlation with tumor cell density and percentage Gleason pattern on whole mount pathology

Daniel I. Glazer,¹ Elmira Hassanzadeh,¹ Andriy Fedorov,¹ Olutayo I. Olubiya,¹ Shayna S. Goldberger,¹ Tobias Penzkofer,² Trevor A. Flood,^{3,4} Paul Masry,⁵ Robert V. Mulkern,⁶ Michelle S. Hirsch,⁷ Clare M. Tempany,¹ Fiona M. Fennessy^{1,8}

¹Department of Radiology, Brigham and Women's Hospital, Boston, MA 02115, USA

²Department of Radiology, Charité University Hospital, Berlin, Germany

³Division of Anatomical Pathology, The Ottawa Hospital, Ottawa, ON K1H 8L6, Canada

⁴University of Ottawa, Ottawa, ON K1H 8L6, Canada

⁵Department of Pathology, Humber River Hospital, Toronto, ON M3M 0B2, Canada

⁶Department of Radiology, Boston Children's Hospital, Boston, MA 02115, USA

⁷Department of Pathology, Brigham and Women's Hospital, Boston, MA, USA

⁸Department of Radiology, Dana Farber Cancer Institute, Boston, MA 02115, USA

Abstract

Objective: To determine if tumor cell density and percentage of Gleason pattern within an outlined volumetric tumor region of interest (TROI) on whole-mount pathology (WMP) correlate with apparent diffusion coefficient (ADC) values on corresponding TROIs outlined on pre-operative MRI.

Methods: Men with biopsy-proven prostate adenocarcinoma undergoing multiparametric MRI (mpMRI) prior to prostatectomy were consented to this prospective study. WMP and mpMRI images were viewed using 3D Slicer and each TROI from WMP was contoured on the high b-value ADC maps (b0, 1400). For each TROI outlined on WMP, TCD (tumor cell density) and the percentage of Gleason pattern 3, 4, and 5 were recorded. The ADC_{mean}, ADC_{10th percentile}, ADC_{90th percentile}, and ADC_{ratio} were also calculated in each case from the ADC maps using 3D Slicer.

Results: Nineteen patients with 21 tumors were included in this study. ADC_{mean} values for TROIs were 944.8 ± 327.4 vs. 1329.9 ± 201.6 mm²/s for adjacent non-neoplastic prostate tissue ($p < 0.001$). ADC_{mean}, ADC_{10th percentile}, and ADC_{ratio} values for higher grade

tumors were lower than those of lower grade tumors (mean 809.71 and 1176.34 mm²/s, $p = 0.014$; 10th percentile 613.83 and 1018.14 mm²/s, $p = 0.009$; ratio 0.60 and 0.94, $p = 0.005$). TCD and ADC_{mean} ($\rho = -0.61$, $p = 0.005$) and TCD and ADC_{10th percentile} ($\rho = -0.56$, $p = 0.01$) were negatively correlated. No correlation was observed between percentage of Gleason pattern and ADC values.

Conclusion: DWI MRI can characterize focal prostate cancer using ADC_{ratio}, ADC_{10th percentile}, and ADC_{mean}, which correlate with pathological tumor cell density.

Key words: Prostate cancer—MRI—ADC—DWI—Gleason pattern

Prostate adenocarcinoma is the most common non-cutaneous malignancy diagnosed in men with over 180,000 cases expected in the United States alone in 2016 [1]. Despite this high incidence, there remains considerable controversy regarding screening, detection, diagnosis, and treatment selection as well as uncertainty regarding the benefit of prostatectomy or early intervention in low-risk patients [2, 3]. It is crucial to attempt to prospectively identify men with clinically insignificant disease

who may be candidates for active surveillance and those with low-to-intermediate risk clinically significant cancers who would benefit from curative treatment, since surgery and radiation therapy carry a significant risk of morbidity, including incontinence and erectile dysfunction [4–7].

Risk stratification of men is complicated by the significant biologic heterogeneity of prostate cancer. Disease-free survival and risk of metastases vary greatly between lower grade (Gleason 3 + 3 and 3 + 4) and higher grade (Gleason 4 + 3 and above) cancer and between Gleason pattern 3 + 4 and Gleason pattern 4 + 3 tumors [8–11]. Consequently, several authors have proposed modified scoring systems based on a quantitative Gleason grade in which the percentage of each pattern is reported or alternative grading systems such as the Prostate Cancer Prevention Trial Risk Calculator so as to more accurately reflect prognosis and reduce overtreatment [12–14].

Alternative pathological findings beyond and in addition to the dominant Gleason pattern may be useful in more accurate prediction of outcome. Indeed, the presence of a cribriform pattern at pathology may portend a worse prognosis regardless of the dominant Gleason pattern [15, 16]. An additional diagnostic shortcoming is that prostate cancer is typically diagnosed by transrectal ultrasound-guided biopsy, which utilizes a random systematic non-targeted sampling pattern. Recent literature has shown that using MRI to pre-define biopsy targets results in larger percentages of high-grade tumor and a more accurate reflection of final pathology [17, 18]. Given the limitations of Gleason scoring and non-targeted prostate biopsies, significant efforts have been made to identify imaging biomarkers that can be used to predict prostate cancer aggressiveness.

Multiparametric prostate MRI (mpMRI) is rapidly becoming a frequently used tool for the detection and diagnosis of prostate cancer, following men on active surveillance, assessing treatment response, and staging known prostate cancer [10]. mpMRI provides an assessment of focal lesions as well as anatomic information using multiple imaging parameters including diffusion-weighted imaging (DWI), T2-weighted images, and dynamic contrast-enhanced imaging. These sequences are strongly suggested in the relative new Prostate Imaging–Reporting and Data System (PI–RADS) v2, which is recommended for the detection of clinically significant disease in treatment-naïve patients. Clinically significant disease is defined as Gleason score ≥ 7 , volume ≥ 0.5 cc, and/or extraprostatic extension [19].

To this end, the apparent diffusion coefficient (ADC) value as calculated from DWI has been investigated and validated as a viable quantifiable metric for determining tumor aggressiveness [20–25]. However, to the best of our knowledge, correlation between ADC metrics and the following pathological features has not yet been

evaluated: (1) the amount of normal tissue interspersed within an area of tumor, (2) the presence of cribriform pattern carcinoma, seen in Gleason pattern 4, and (3) the tertiary Gleason grade of the tumor.

The typical approach to date, to measuring ADC, has been to identify the lesion on DWI, select a central slice, and place a region of interest (ROI) on the single slice to obtain a planar ADC measurement. In fact, PI–RADSv2 does not require a quantitative metric, relying on a qualitative assessment of low ADC or restricted diffusion. A less frequently used approach is to assess the entire lesion by whole-lesion volumetric assessment of quantitative ADC parameters. It has been proposed that this latter method is better for separating low-grade from high-grade tumors [26, 27], and is superior because of the significant heterogeneity of prostate cancer within a given area of the tumor that could potentially lead to erroneous characterization based on a single ROI image ADC measurement [26]. Rosenkrantz et al. demonstrated that there is, indeed, a correlation between ADC entropy within a volumetric outlined tumor and percentage of Gleason pattern 4 cancer within Gleason 7 tumors at radical prostatectomy [27].

The purpose of our study was to determine whether the tumor cell density (TCD) and percentage of Gleason pattern within an outlined volumetric tumor region of interest (TROI) on whole-mount pathology (WMP) slides correlate with extracted ADC values on corresponding TROIs outlined on pre-operative MRI.

Materials and methods

The local institutional review board approved the study, and written informed consent was prospectively obtained from all patients. The study was compliant with the Health Insurance Portability and Accountability Act.

Patients

The study was prospective in nature with patients enrolled at the time of mpMRI. To be included in the study, patients were required to have a tissue diagnosis of prostate cancer, an elevated serum prostate-specific antigen (PSA) measured within 6 weeks prior to MR imaging, be able to undergo an endorectal coil prostate 3T MR, and be scheduled for radical prostatectomy as their treatment strategy. In addition, patients were required to consent to whole-mount pathological analysis of the prostate following radical prostatectomy. Time from mpMRI to MRI-guided prostate biopsy was recorded.

Patients were excluded if they did not have an endorectal coil prostate MRI, did not consent to WMP analysis, or were planning any treatment other than radical prostatectomy. Two of our previous studies reported on this cohort of patients who underwent whole-

mount pathology, but did not report any volumetric ADC analysis or detailed correlation between tumor cell density and whole-mount pathology [28, 29].

Multiparametric MRI

All studies were performed using the same magnet (3.0 T GE Signa HDx MRI scanner, GE Healthcare, Waukesha, WI). A body coil was used for excitation, and an eight channel abdominal array and an endorectal coil filled with air (Medrad, Pittsburgh, PA) were used for signal reception. The mpMRI protocol consisted of: T1-weighted imaging [spoiled gradient recalled acquisition in steady state (SPGR) sequence, repetition time (TR)/echo time (TE)/ $\alpha = 385$ ms/6.2 ms/65°, over a 16 cm² field of view (FOV)]; T2-weighted imaging (fast relaxation fast spin echo (FRFSE) sequence, TR/TE = 3500 ms/102 ms over a 16 cm² FOV); DWI imaging [single-shot echo planar imaging (EPI) sequence, TR/TE = 2500 ms/65 ms with b values of 500 and 1400 s/mm²]; and dynamic contrast-enhanced imaging (3D SPGR sequence, TR/TE/ $\alpha = 3.6$ ms/1.3 ms/15°, FOV 26 cm) [30]. Dynamic contrast-enhanced sequences were obtained following Gadopentetate dimeglumine (Magnevist; Berlex Laboratories, Wayne, NJ) intravenous injection using a syringe pump (0.15 mmol/kg; rate 3 mL/s).

Histopathology acquisition and analysis

All radical prostatectomy specimens were inked for laterality and fixed overnight in 40% buffered formalin at room temperature. The first 26 consecutive specimens were sectioned manually from apex to base at 4–5 mm intervals. A customized 3D mold of the prostate was used with the subsequent four specimens to achieve a constant slice thickness of 3 mm [31]. Each slice was marked accordingly for tissue orientation, annotated by slice number, fixed, and then paraffin embedded. Subsequently, 5-micron whole-mount sections were cut from the paraffin-embedded tissue, mounted on glass slides, and stained with hematoxylin and eosin. The interface of the peripheral zone and transition zone and all cancer foci were outlined with a marker on the glass slides by a genitourinary pathologist with more than 10 years' experience (MSH). Each cancer focus was assigned a Gleason score, calculated as the most predominant Gleason pattern plus the second most predominant Gleason pattern. A third Gleason pattern representing a minor tertiary component was included as a third grade if and when present. Additionally, the estimated percent of Gleason patterns 3, 4, and 5 and the TCD (as determined by the percent volume of tumor cells compared to non-neoplastic tissues in the same area) were documented. TROIs were contoured manually on the WMP slides by the pathologist. The annotated WMP slides

were then digitally scanned and loaded into 3D Slicer (<http://slicer.org>), an open-source software for medical image visualization and analysis [32]. Tumor volumes were automatically calculated based on these manual contours and assuming a 5 mm slice thickness for routine WMP processing and a 3 mm slice for processing using the customized mold. According to the methods of Jonmarker et al., tumor volumes were scaled by a factor of 1.15 to correct for tissue shrinkage during processing [33].

Correlation of MR images with histopathology and image processing

Correlation between whole-mount pathology and MR images was performed only in patients with clinically significant tumors, defined as an index tumor focus ≥ 0.50 cc [34, 35]. Annotated WMP and mpMRI images were viewed side-by-side in 3D Slicer and reviewed in consensus by a genitourinary (GU) pathologist and two GU radiologists with more than 10 and 2 years' experience, respectively, in interpreting prostate MRI (MSH, FMF, TP). Direct visual correlation was made between the WMP images and the MR images for accurate delineation of tumor on MRI. However, at the time of tumor contouring on MR, the radiologists were blinded to quantitative pathology metrics. Utilizing anatomic landmarks for guidance, the contoured TROIs from the digital pathology slides were mapped to the mpMRI datasets. All mpMRI sequences were used to confirm lesion location. Using the volumetric TROI generated in 3D Slicer, the ADC_{mean}, ADC_{10th percentile} (mean value of the pixels in the lower 10% of the distribution), and the ADC_{90th percentile} (mean value of the pixels in the top 10% of the distribution) were measured. A region of interest was also contoured in adjacent non-neoplastic prostatic tissue (NNPT) from the same zone (when possible, on the same axial image) to allow for calculation of an ADC_{ratio} (tumor ADC_{mean}/NNPT ADC_{mean}).

Statistical analysis

Standard summary statistics were used to present the baseline patient and lesion characteristics. ADC_{mean} values of the segmented tumor and adjacent normal parts of the prostate were compared using a paired t test; a two sample t test was used to compare ADC values of "high-grade" versus "low-grade" tumors. Only two-sided p values at preset significant (alpha) value of ≤ 0.05 were reported. Spearman's correlation coefficient " ρ " was calculated for comparing the relationship between ADC metrics (ADC_{mean}, ADC_{ratio}, ADC_{90th percentile}, and ADC_{10th percentile}) and whole-mount pathology analyses (TCD and percentage of individual Gleason pattern). All analyses were performed using Stata version 11.2 (StataCorp LP, College Station, TX).

Results

Study population

Thirty male patients (mean age 60 years; range 45–69 years) with biopsy-proven prostate adenocarcinoma prospectively consented to participate in the study from February 2010 to May 2013. The mean PSA was 6.7 ng/ml (2.2–25.95) and the mean time from MRI to prostatectomy was 58 days (10–217). Eleven of these 30 men were subsequently excluded for the following reasons: no index tumor >0.5 cc at final pathology ($n = 8$), extensive hemorrhage limiting visualization of the tumor ($n = 2$), and insufficient image quality ($n = 1$). The mean age of the remaining 19 patients included in the final analyses was 60.6 years (45–69), the mean PSA was 6.7 mg/dl (2.2–25.95), and the mean time between MRI and prostatectomy was 55 days (10–217).

Pathology results

The majority of the 21 included tumors (19 patients had a single index tumor >0.5 cc and two patients had two tumors >0.5 cc) were located in the peripheral zone ($n = 17$) with a small number of tumors in the transition zone ($n = 4$). The mean corrected tumor volume was 2.1 cc (0.56–7.0) and the mean TCD within each defined tumor volume was 68.6% (30–90). Eight tumors were lower grade (3 + 3 and 3 + 4) and 13 tumors were higher grade (3 + 4 + 5, 4 + 3, and 4 + 3 + 5) (Table 1). The median percentage of Gleason pattern 3 was 50% (10–100), the median percentage of pattern 4 was 40% (0–80), and the median percentage of pattern 5 was 0% (0–15) (Table 1). A cribriform pattern was present in 25% of tumors (5/20) that had Gleason pattern 4 disease.

Table 1. Summary of Gleason scores, tumor volume, and tumor cell density for all tumors based on whole-mount pathology ($n = 21$)

Distribution of Gleason scores	
3 + 3	1
3 + 4	7
3 + 4 + 5	2
4 + 3	7
4 + 3 + 5	4

Parameter	Value
Mean corrected tumor volume (cc)	2.1 (0.56–7.0)
TCD in TROI (%)	68.6 (30–90)
Median percentage Gleason pattern 3	50 (10–100)
Median percentage Gleason pattern 4	40 (0–80)
Median percentage Gleason pattern 5	0 (0–15)

Gleason scores are calculated as the most predominant plus the second most predominant Gleason pattern; a third grade represents the presence of a tertiary Gleason pattern when present
TCD tumor cell density, *TROI* tumor region of interest

ADC values

The ADC_{mean} value for tumors was consistently lower than in adjacent non-neoplastic prostate tissue (944.8 vs 1329.9 mm^2/s , $p = 0.0004$) (Table 2; Fig. 1). ADC_{10th} percentile value for tumors was 762.8 mm^2/s and ADC_{90th} percentile value for tumors was 1124.9 mm^2/s (Table 2). The mean ADC_{ratio} was 0.72 (Table 2).

Correlation of ADC with tumor cell density

ADC_{mean} , ADC_{10th} percentile, and ADC_{ratio} values all decreased as tumor cell density within a TROI at WMP increased. The strongest negative correlation with TCD within a given volume was observed with ADC_{mean} ($\rho = -0.61$, $p = 0.005$) (Table 3; Fig. 2). ADC_{10th} percentile also demonstrated a strong correlation with TCD ($\rho = -0.5570$, $p = 0.01$) (Table 3). Finally, there was a statistically significant correlation between ADC_{ratio} and TCD ($\rho = -0.465$, $p = 0.04$) (Table 3).

Relationship of ADC values with Gleason sum score and individual Gleason pattern

When tumors were divided into lower [Gleason 3 + 3 and 3 + 4 ($n = 8$)] and higher grade [Gleason

Table 2. Summary of tumor and non-neoplastic prostate tissue ADC measurements

ADC parameter	Value
Tumor ADC_{10th} percentile	762.8 mm^2/s (422–1677)
Tumor ADC_{mean}	944.8 mm^2/s (641.3–1854.4)
Tumor ADC_{90th} percentile	1124.9 mm^2/s (853–1984)
Tumor ADC_{ratio}	0.72 (0.48–1.6)
NNPT ADC_{mean}	1329.9 mm^2/s (1153.5–2033.8)

NNPT non-neoplastic prostate tissue

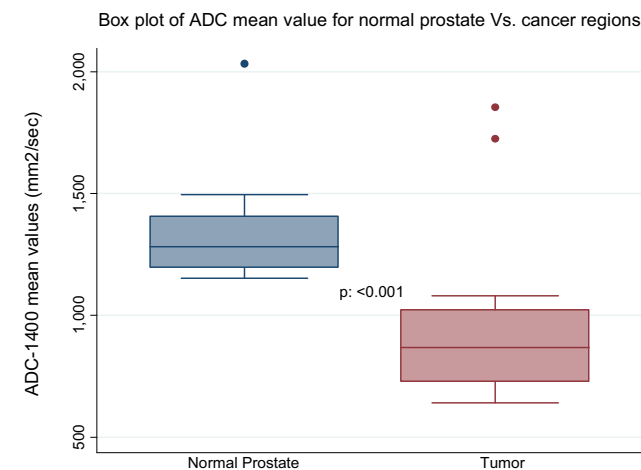


Fig. 1. ADC_{mean} values for normal prostate and tumor regions of interest.

3 + 4 + 5, 4 + 3, 4 + 3 + 5 ($n = 13$) tumors, the difference in ADC values between these two groups was significant for ADC_{mean} (1176.34 and 809.71 mm^2/s , $p = 0.014$), $ADC_{10th\ percentile}$ (1018.14 and 613.83 mm^2/s , $p = 0.009$), and ADC_{ratio} (0.94 and 0.60, $p = 0.005$) (Table 4; Fig. 3). There was a trend toward inverse correlation between decreasing $ADC_{90th\ percentile}$ and ADC_{ratio} values ($\rho = -0.4218$, $p = 0.07$ and $\rho = -0.4197$, $p = 0.07$, respectively) and increasing percentage of Gleason pattern 4 tumor within a given TROI that was not statistically significant (Table 5). There was also a trend between increasing $ADC_{90th\ percentile}$ values and an increasing percentage of Gleason pattern 3 tumor within a given TROI ($\rho = 0.4292$, $p = 0.07$), that also was not statistically significant (Table 5). The presence of a cribriform pattern was not correlated with ADC values. A representative cross section of the gross pathology specimen, a whole-mount H&E-stained section, and corresponding MRI images are shown in Fig. 4.

Discussion

We report for the first time that there is an inverse correlation between volumetric whole-lesion quantitative ADC parameters and tumor cell density obtained from whole-mount radical prostatectomy pathologic analysis. Tumor ADC values were significantly lower than normal

Table 3. Correlation between ADC values and tumor cell density within a tumor region of interest

ADC parameter	Correlation with TCD within a given TROI	p value
ADC_{mean}	$\rho = -0.6164$	0.005
$ADC_{10th\ percentile}$	$\rho = -0.5570$	0.01
ADC_{ratio}	$\rho = -0.4650$	0.04

ADC_{ratio} tumor $ADC_{mean}/NNPT\ ADC_{mean}$, $NNPT$ non-neoplastic prostate tissue

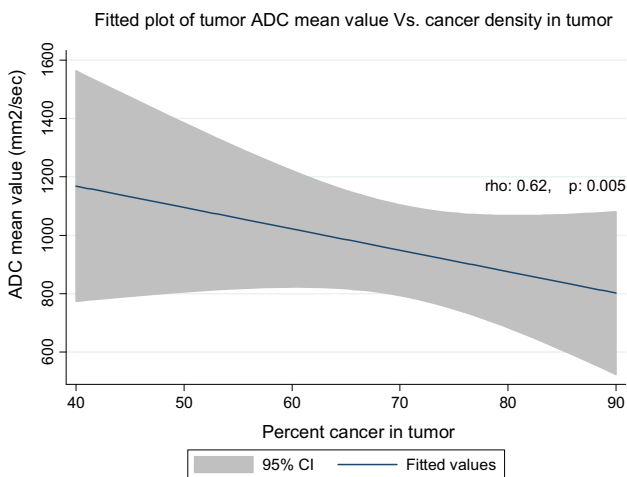


Fig. 2. Correlation between ADC_{mean} value and tumor cell density.

prostate ADC values. Higher grade tumors had significantly lower ADC values than lower grade tumors. No correlation was observed between the percentage of Gleason pattern 3 and 4 tumor in a TROI and volumetric ADC values or between the presence of cribriform pattern and ADC values.

While TCD is not directly associated with Gleason score, it has been associated with increasing tumor aggressiveness and neuroendocrine differentiation [36, 37]. Given the relationship between quantitative ADC parameters, Gleason score and TCD use of these measurements to prospectively triage men into a lower or

Table 4. Comparison of ADC values for lower and higher grade tumors

ADC parameter	Lower grade ($n = 8$)	Higher grade ($n = 13$)	p value
$ADC_{10th\ percentile}$	1018.14 mm^2/s	613.83 mm^2/s	0.009
ADC_{mean}	1176.34 mm^2/s	809.71 mm^2/s	0.014
$ADC_{90th\ percentile}$	1341 mm^2/s	998.83 mm^2/s	0.013
ADC_{ratio}	0.94	0.60	0.005

ADC_{ratio} (tumor $ADC_{mean}/NNPT\ ADC_{mean}$)

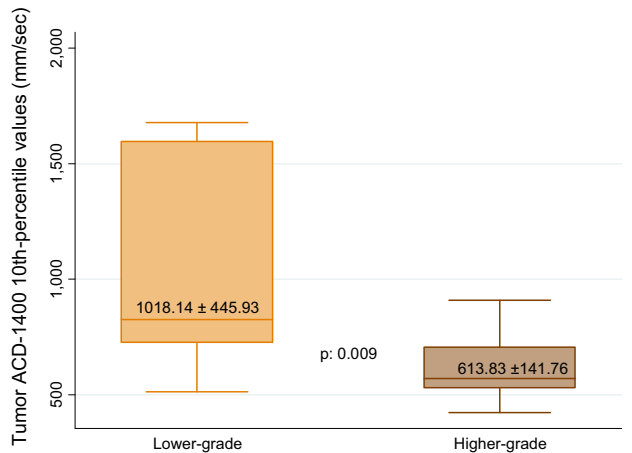
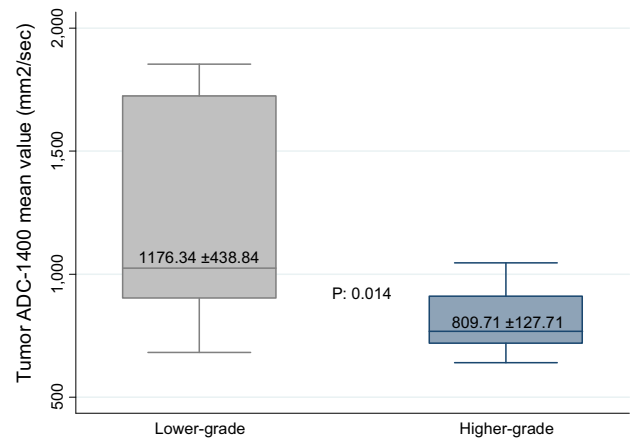


Fig. 3. ADC_{mean} and $ADC_{10th\ percentile}$ values comparison of lower versus higher grade prostate cancer. Lower grade Gleason 3 + 3 and 3 + 4; Higher grade Gleason 3 + 4 + 5, 4 + 3, and 4 + 3 + 5.

Table 5. Correlation between ADC values and percentage of individual Gleason patterns within a tumor region of interest

ADC Parameter	Correlation with % Gleason pattern 3	<i>p</i> value	Correlation with % Gleason pattern 4	<i>p</i> value
ADC _{10th percentile}	0.3116	0.19	-0.3141	0.19
ADC _{mean}	0.4022	0.09	-0.4082	0.09
ADC _{90th percentile}	0.4365	0.06	-0.4218	0.07
ADC _{ratio}	0.4292	0.07	-0.4197	0.07

Lower grade Gleason 3 + 3 and 3 + 4, *Higher grade* Gleason 3 + 4 + 5, 4 + 3, and 4 + 3 + 5
 ADC_{ratio} tumor ADC_{mean}/NNPT ADC_{mean}, TCD tumor cell density

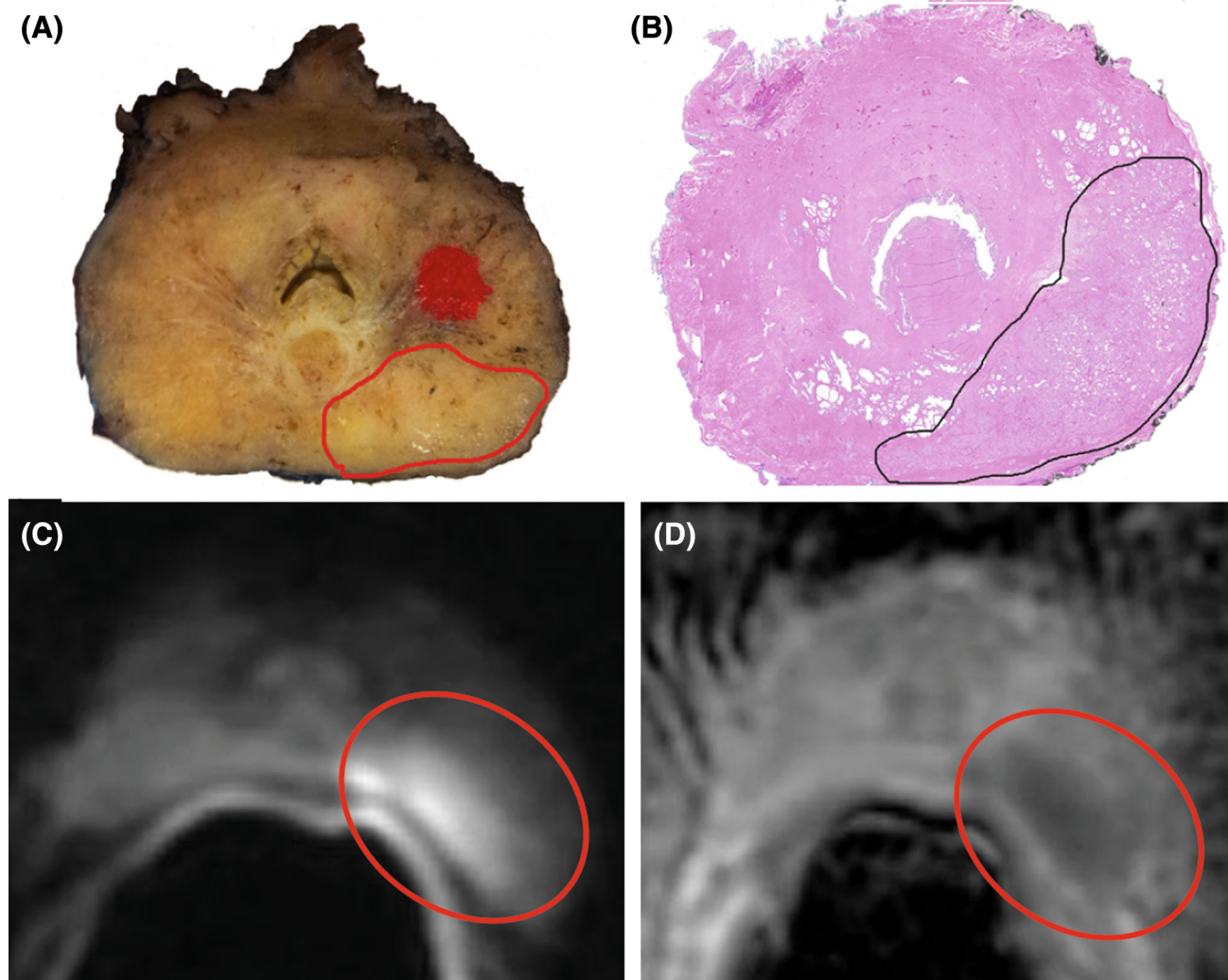


Fig. 4. Gross, histologic, and MRI images from a single patient with 3 + 4 = 7 prostate adenocarcinoma. **A** Complete gross cross section of the prostate (slice 3); the area of carcinoma in the *left posterior* is demarcated by an *open red circle* (note, the *red solid dot* is a designation mark used to ensure that all sections of the prostate were embedded and

sectioned with the same orientation). **B** A complete H&E-stained cross section of the prostate (*slide 4*); the area of carcinoma in the *left posterior* is demarcated by an *open black circle*. **C** DWI image. **D** ADC map; the tumor appears hyperintense on high b-value diffusion-weighted image (*red circle*), and hypointense on corresponding ADC map (*red circle*).

higher risk category for cancer recurrence/progression based principally on the pre-prostatectomy mpMRI results should be further explored. This distinction between low- and high-grade diseases is clinically important as men with more aggressive cancers have an increased risk

of biochemical failure following prostatectomy, systemic recurrence, and prostate cancer mortality [38]. Additionally, mpMRI may also be able to prospectively distinguish between clinically significant and clinically insignificant prostate adenocarcinoma [39]. Therefore,

mpMRI may serve as an imaging biomarker to aid in differentiating high-grade from low-grade prostate cancer prior to surgery, and potentially impact treatment decisions and patient expectations following therapy. While tumor cell density is not currently used clinically, its use as a quantitative pathology biomarker in future correlative studies should be explored.

The negative correlation between ADC value and tumor cellularity has been previously described and attributed to differences in cellularity between normal prostatic tissue and prostate cancer and the resulting effects on diffusivity of water [40, 41]. However, a study by Chatterjee et al. suggests that the differences in diffusivity are more influenced by differences in the relative volumes of prostate glandular components (i.e., varying amounts of epithelial structures, stroma, inflammation, blood vessels, etc.) than by conventionally cited cellularity metrics [42]. Regardless of the exact mechanism, there remains an association between decreasing ADC and tumor aggressiveness.

Our results regarding the importance of ADC in determining prostate cancer aggressiveness are in accord with multiple other studies [20, 26, 43, 44]. The value of ADC in prostate cancer detection and determination of aggressiveness was previously demonstrated in both the central gland [25] and the peripheral zone [23]. In addition to ADC_{mean} , $ADC_{10\text{th percentile}}$ has been proposed as a biomarker for tumor aggressiveness as this value may reflect the highest grade tumor found in a given lesion [26]. Our results add the correlation between ADC values and tumor cell density and support this conclusion. Finally, a study by Boesen et al. also confirmed the inverse relationship between ADC and Gleason score at radical prostatectomy, but further found that ADC_{ratio} was superior to the ADC_{mean} alone [22]. We did observe that ADC_{ratio} correlated negatively with increasing TCD and was also lower in higher grade tumors.

Limitations

The number of lesions and patients used in the study was small as we evaluated only 21 tumors in 19 patients. It should also be noted that WMP is not routinely performed at our institution and was implemented specifically for the purposes of this study. Therefore, we purposely chose to avoid a retrospective pathological correlation study using quadrant tissue mounts as tumor localization and volume estimation accuracy are compromised in such data [28]. Only a small minority of the prostate cancers demonstrated a cribriform pattern ($n = 5$), which may have affected the results. ROIs were drawn in consensus, which could have introduced some bias although the radiologists were not aware of the detailed pathology results at the time of contouring. Only a single pathologist reviewed the prostatectomy specimens, and interobserver variation in Gleason grading is

possible. Further, we deliberately evaluated only those patients who had index tumors larger than 0.5 cc in order to ensure a substantive tumor volume for image and pathological analysis as well as to focus on clinically significant prostate cancer.

Summary

We observed an inverse correlation between ADC parameters— ADC_{mean} , $ADC_{10\text{th percentile}}$, and ADC_{ratio} —and tumor cell density within a given tumor volume. ADC_{mean} , $ADC_{10\text{th percentile}}$, and ADC_{ratio} values were lower in higher grade tumors than in lower grade tumors. No correlation was seen between percentage of Gleason pattern 3 and 4 tumor within a TROI and ADC value. Exploration of volumetric ADC parameters holds potential for helping guide men to the most appropriate treatment strategy and allow resources to be concentrated on treating more aggressive and higher grade cancers. Prostate diffusion-weighted MRI can characterize focal prostate cancer using ADC_{ratio} , $ADC_{10\text{th percentile}}$, and ADC_{mean} , which correlate with pathological tumor cell density and therefore may explain the underlying pathophysiology of ADC measurements.

Acknowledgments. The authors thank Louise Greenberg, M.Ed. for coordination of this study and Nina Geller Ph.D. for editing assistance.

Grant Support. Grant funding was provided by U01CA151261 (FMF, AF), U24CA180918 (AF), R25CA89017 (DIG), P41EB015898 (CT, FF, AF), and DPH403516 (EH).

Compliance with Ethical Standards

Conflict of Interest None.

Ethical approval The study was HIPAA compliant and approved by the Institutional Review Board. Informed consent was obtained from all individual participants included in the study. All procedures performed in studies involving human participants were in accordance with the ethical standards of the institutional and/or national research committee, and with the 1964 Helsinki declaration and its later amendments or comparable ethical standards.

References

1. Cancer Facts & Figures (2016) American Cancer Society, Atlanta
2. Wilt TJ, Brawer MK, Jones KM, et al. (2012) Radical prostatectomy versus observation for localized prostate cancer. *N Engl J Med* 367(3):203–213
3. Hamdy FC, Donovan JL, Lane JA, et al. (2016) 10-Year outcomes after monitoring, surgery, or radiotherapy for localized prostate cancer. *N Engl J Med*. doi:10.1056/NEJMoa1606221
4. Dinh KT, Mahal BA, Ziehr DR, et al. (2015) Incidence and predictors of upgrading and up staging among 10,000 contemporary patients with low risk prostate cancer. *J Urol* 194(2):343–349
5. Dinh KT, Muralidhar V, Mahal BA, et al. (2015) Occult high-risk disease in clinically low-risk prostate cancer with $\geq 50\%$ positive biopsy cores: should national guidelines stop calling them low-risk? *Urology*. doi:10.1016/j.urology.2015.08.026
6. Barry MJ, Gallagher PM, Skinner JS, Fowler FJ (2012) Adverse effects of robotic-assisted laparoscopic versus open retropubic

- radical prostatectomy among a nationwide random sample of medicare-age men. *J Clin Oncol* 30(5):513–518
7. Ploussard G, Epstein JI, Montironi R, et al. (2011) The contemporary concept of significant versus insignificant prostate cancer. *Eur Urol* 60(2):291–303
 8. Stark JR, Perner S, Stampfer MJ, et al. (2009) Gleason score and lethal prostate cancer: does $3 + 4 = 4 + 3$? *J Clin Oncol* 27(21):3459–3464
 9. Hricak H, Choyke PL, Eberhardt SC, Leibel SA, Scardino PT (2007) Imaging prostate cancer: a multidisciplinary perspective. *Radiology* 243(1):28–53
 10. Turkbey B, Brown AM, Sankineni S, Wood BJ, Pinto PA, et al. (2015) Multiparametric prostate magnetic resonance imaging in the evaluation of prostate cancer. *CA Cancer J Clin* 40(7):2557–2565
 11. Glazer DI, Davenport MS, Khalatbari S, et al. (2015) Mass-like peripheral zone enhancement on CT is predictive of higher-grade (Gleason 4 + 3 and higher) prostate cancer. *Abdom Imaging* 40(3):560–570
 12. Epstein JI, Zelefsky MJ, Sjoberg DD, et al. (2015) A contemporary prostate cancer grading system: a validated alternative to the gleason score. *Eur Urol* . doi:[10.1016/j.eururo.2015.06.046](https://doi.org/10.1016/j.eururo.2015.06.046)
 13. Sauter G, Steurer S, Clauditz TS, et al. (2015) Clinical utility of quantitative gleason grading in prostate biopsies and prostatectomy specimens. *Eur Urol* . doi:[10.1016/j.eururo.2015.10.029](https://doi.org/10.1016/j.eururo.2015.10.029)
 14. Ankerst DP, Hoefler J, Bock S, et al. (2014) Prostate cancer prevention trial risk calculator 2.0 for the prediction of low- vs high-grade prostate cancer. *Urology* 83(6):1362–1367
 15. Kweldam CF, Wildhagen MF, Steyerberg EW, Bangma CH, van der Kwast TH, van Leenders GJ (2015) Cribriform growth is highly predictive for postoperative metastasis and disease-specific death in Gleason score 7 prostate cancer. *Mod Pathol* 28(3):457–464
 16. Dong F, Yang P, Wang C, et al. (2013) Architectural heterogeneity and cribriform pattern predict adverse clinical outcome for Gleason grade 4 prostatic adenocarcinoma. *Am J Surg Pathol* 37(12):1855–1861
 17. Radtke JP, Schwab C, Wolf MB, et al. (2016) Multiparametric magnetic resonance imaging (MRI) and MRI-transrectal ultrasound fusion biopsy for index tumor detection: correlation with radical prostatectomy specimen. *Eur Urol* . doi:[10.1016/j.eururo.2015.12.052](https://doi.org/10.1016/j.eururo.2015.12.052)
 18. Delongchamps NB, Lefèvre A, Bouazza N, Beuvon F, Legman P, Cornud F (2015) Detection of significant prostate cancer with magnetic resonance targeted biopsies—should transrectal ultrasound-magnetic resonance imaging fusion guided biopsies alone be a standard of care? *J Urol* 193(4):1198–1204
 19. Weinreb JC, Barentsz JO, Choyke PL, et al. (2016) PI-RADS Prostate Imaging—Reporting and Data System: 2015, Version 2. *Eur Urol* 69(1):16–40
 20. Vargas HA, Akin O, Franiel T, et al. (2011) Diffusion-weighted endorectal MR imaging at 3 T for prostate cancer: tumor detection and assessment of aggressiveness. *Radiology* 259(3):775–784
 21. Kim TH, Jeong JY, Lee SW, et al. (2015) Diffusion-weighted magnetic resonance imaging for prediction of insignificant prostate cancer in potential candidates for active surveillance. *Eur Radiol* 25(6):1786–1792
 22. Boesen L, Chabanova E, Løgager V, Balslev I, Thomsen HS (2015) Apparent diffusion coefficient ratio correlates significantly with prostate cancer gleason score at final pathology. *J Magn Reson Imaging* 42(2):446–453
 23. Hambrock T, Somford DM, Huisman HJ, et al. (2011) Relationship between apparent diffusion coefficients at 3.0-T MR imaging and Gleason grade in peripheral zone prostate cancer. *Radiology* 259(2):453–461
 24. Mazaheri Y, Shukla-Dave A, Hricak H, et al. (2008) Prostate cancer: identification with combined diffusion-weighted MR imaging and 3D 1H MR spectroscopic imaging—correlation with pathologic findings. *Radiology* 246(2):480–488
 25. Oto A, Kayhan A, Jiang Y, et al. (2010) Prostate cancer: differentiation of central gland cancer from benign prostatic hyperplasia by using diffusion-weighted and dynamic contrast-enhanced MR imaging. *Radiology* 257(3):715–723
 26. Donati OF, Mazaheri Y, Afaq A, et al. (2014) Prostate cancer aggressiveness: assessment with whole-lesion histogram analysis of the apparent diffusion coefficient. *Radiology* 271(1):143–152
 27. Rosenkrantz AB, Triolo MJ, Melamed J, Rusinek H, Taneja SS, Deng FM (2015) Whole-lesion apparent diffusion coefficient metrics as a marker of percentage Gleason 4 component within Gleason 7 prostate cancer at radical prostatectomy. *J Magn Reson Imaging* 41(3):708–714
 28. Fedorov A, Penzkofer T, Hirsch MS, et al. (2015) The role of pathology correlation approach in prostate cancer index lesion detection and quantitative analysis with multiparametric MRI. *Acad Radiol* 22(5):548–555
 29. Fennessy FM, Fedorov A, Penzkofer T, et al. (2015) Quantitative pharmacokinetic analysis of prostate cancer DCE-MRI at 3T: comparison of two arterial input functions on cancer detection with digitized whole mount histopathological validation. *Magn Reson Imaging* 33(7):886–894
 30. Hegde JV, Mulker RV, Panych LP, et al. (2013) Multiparametric MRI of prostate cancer: an update on state-of-the-art techniques and their performance in detecting and localizing prostate cancer. *J Magn Reson Imaging* 37(5):1035–1054
 31. Trivedi H, Turkbey B, Rastinehad AR, et al. (2012) Use of patient-specific MRI-based prostate mold for validation of multiparametric MRI in localization of prostate cancer. *Urology* 79(1):233–239
 32. Fedorov A, Beichel R, Kalpathy-Cramer J, et al. (2012) 3D Slicer as an image computing platform for the Quantitative Imaging Network. *Magn Reson Imaging* 30(9):1323–1341
 33. Jonmarker S, Valdman A, Lindberg A, Hellström M, Egevad L (2006) Tissue shrinkage after fixation with formalin injection of prostatectomy specimens. *Virchows Arch* 449(3):297–301
 34. Stamey TA, Freiha FS, McNeal JE, et al. (1993) Localized prostate cancer. Relationship of tumor volume to clinical significance for treatment of prostate cancer. *Cancer* 71(3 Suppl):933–938
 35. Wolters T, Roobol MJ, van Leeuwen PJ, et al. (2011) A critical analysis of the tumor volume threshold for clinically insignificant prostate cancer using a data set of a randomized screening trial. *J Urol* 185(1):121–125
 36. Kuwano H, Miyazaki T, Tsutsumi S, et al. (2004) Cell density modulates the metastatic aggressiveness of a mouse colon cancer cell line, colon 26. *Oncology* 67(5–6):441–449
 37. Pernicová Z, Slabáková E, Fedr R, et al. (2014) The role of high cell density in the promotion of neuroendocrine transdifferentiation of prostate cancer cells. *Mol Cancer* 13:113
 38. Tollefson MK, Leibovich BC, Slezak JM, Zincke H, Blute ML (2006) Long-term prognostic significance of primary Gleason pattern in patients with Gleason score 7 prostate cancer: impact on prostate cancer specific survival. *J Urol* 175(2):547–551
 39. Vargas HA, Hötter AM, Goldman DA, et al. (2015) Updated prostate imaging reporting and data system (PI-RADS v2) recommendations for the detection of clinically significant prostate cancer using multiparametric MRI: critical evaluation using whole-mount pathology as standard of reference. *Eur Radiol* . doi:[10.1007/s00330-015-4015-6](https://doi.org/10.1007/s00330-015-4015-6)
 40. Gibbs P, Liney GP, Pickles MD, Zelhof B, Rodrigues G, Turnbull LW (2009) Correlation of ADC and T2 measurements with cell density in prostate cancer at 3.0 Tesla. *Investig Radiol* 44(9):572–576
 41. Zelhof B, Pickles M, Liney G, et al. (2009) Correlation of diffusion-weighted magnetic resonance data with cellularity in prostate cancer. *BJU Int* 103(7):883–888
 42. Chatterjee A, Watson G, Myint E, et al. (2015) Changes in epithelium, stroma, and lumen space correlate more strongly with Gleason Pattern and are stronger predictors of prostate ADC changes than cellularity metrics. *Radiology* 277(3):751–762
 43. Bollineni VR, Kramer G, Liu Y, Melidis C, deSouza NM (2015) A literature review of the association between diffusion-weighted MRI derived apparent diffusion coefficient and tumour aggressiveness in pelvic cancer. *Cancer Treat Rev* 41(6):496–502
 44. Turkbey B, Shah VP, Pang Y, et al. (2011) Is apparent diffusion coefficient associated with clinical risk scores for prostate cancers that are visible on 3-T MR images? *Radiology* 258(2):488–495